Radiation-Assisted Metal Ion Interference Tumor Therapy by Barium Peroxide-Based nanoparticles

Meng Zhang,[ab] Bo Shen,[c] Ruixue Song,[d] Han Wang,[ab] Bin Lv,[e] Xianfu Meng,[d] Yang Liu,[d] Yanyan Liu,[d] Xiangpeng Zheng,[e] Weiwei Su,[f] Changjing Zuo,*[f] and Wenbo Bu*[ad]

a State Key Laboratory of High Performance Ceramics and Superfine Microstructures, Shanghai Institute of Ceramics, Chinese Academy of Sciences, Shanghai 200050, China

b University of Chinese Academy of Sciences, Beijing 100049, China

c Institute of Radiation Medicine, Fudan University, China

d Shanghai Key Laboratory of Green Chemistry and Chemical Processes, School of Chemistry and Molecular Engineering, East China Normal University, Shanghai 200062, China

e Department of Radiation Oncology, Huadong Hospital, Fudan University, Shanghai, 200040, China

f Department of Nuclear Medicine, Changhai Hospital, Navy Medical University, Shanghai 200433, China

KEYWORDS: barium peroxide; tumor radiotherapy; chelators; hydroxyl radical;

Experimental methods

1. Materials

Barium chloride, sodium formate, choline hydroxide (48-50 wt.% solution in H_2O), and 3 wt.% hydrogen peroxide were gained from J&K Scientific. N, N-bis(carboxymethyl)-L-glutamic acid tetrasodium salt (40 wt.% solution in H_2O) was purchased from TCI chemicals. 5,5-Dimethyl-1-pyrroline N-oxide, Coumarin and HPF was purchased from Sigma-Aldrich. DCFH-DA and cell counting kit-8 was purchased from Yeasen. DiSBAC2(5) was purchased from AAT bioquest®.

2. Characterization

Transmission electron microscopy images (TEM) were gained on the electron microscope (JEM-2100F, 200 kV). X-ray diffraction patterns were acquired on a Rigaku D/MAX-2250V diffractometer. The hydrodynamic radius and zeta-potential were collected on a Nanotrac Wave II Q Nanoparticle Size Analyzer, Microtrac. Fourier transform infrared (FT-IR) spectra were obtained on a Bruker TENSOR II FTIR Spectrometer. Calcium ion concentrations were recorded on an Agilent 5110 ICP-OES. CCK8 assays were conducted on a Spark™ Multimode Microplate Reader. Confocal laser scanning microscopic (CLSM) images were carried out using the Nikon $A1^+R$-980 Confocal Microscope. The cellular statistic calcium fluorescence was measured on a guava easycyte 6HL-2L flow cytometry, Germany.

3. Synthesis of the GL-BaO_2 NPs

The BaO_2 NPs were prepared in a methanol-water mixture at room temperature. Typically, 1 mL sodium formate (1 mol/L) and 0.5 mL $BaCl_2$ (1 mol/L) aqueous solution were ultrasonic mixed together before added into 30 mL of absolute methanol. After vigorously stirring for several minutes, excessive amounts of hydrogen peroxide were dropped into the mixture, following with the addition of 20 μL choline hydroxide aqueous solution. When the colorless system turned into Cambridge blue, the solution was centrifuged and washed twice with methanol before washed another time with methanol/water. The product was finally dispersed in 20 mL ethanol. To investigate the influence of precursor selection on the morphology and size of BaO_2 nanoparticles, sodium formate was replaced with water, citric or EDTA.

For the surface modification, 0.1 mmol of unmodified BaO_2 NPs were re-dispersed in a 90 mL ethanol/water (2:1, volume ratio) solution. Then 10 mL of GLDA (10 mmol/L) was added and stirred for 1 h at room temperature before the centrifugation and washing with ethanol/water. The GLDA modified BaO_2 NPs were finally dispersed in 20 mL ethanol. Besides, changing the initial addition amount of GLDA as 2 mL, 5 mL and 20 mL, we got NPs with varied proportion of modification (The ratio between BaO_2 and GLDA were denote as 5:1, 2:1 and 1:2)

4. Study of the stability of GL-BaO_2 NPs within two weeks

To study the stability of GL-BaO_2 NPs in pH 7.2 buffer, the release of Ba^{2+} and H_2O_2 are evaluated by the dialysis method. Basically, 1 mL of GL-BaO_2 NPs (300 μg/mL) is loaded in a dialysis bag, and then immersed in 15 mL of pH 7.2 buffer. At certain time point within two weeks, 4 mL of buffer is taken out to measure the Ba^{2+} concentration by ICP-MS, followed by the replenishment of 4 mL of fresh buffer. Finally, the percentage of Ba^{2+} leakage is calculated. For measuring the decomposed amount of H_2O_2, 100 μL of sample is taken out each time and recorded with the cerium sulfate reduction method.

5. Detecting the specific free radical ·OH production using Electron paramagnetic resonance (EPR) spectroscopy

5,5-Dimethyl-1-pyrroline N-oxide (DMPO) was employed as a spin trapping agent to detect the enhanced hydroxyl radical production of BaO_2 NPs after the X-ray radiation. Typically, 100 μL of DMPO (100 mM) were mixed with 50 μL of the following reagents before processing with 5 Gy of radiation: i) deionized water; ii) 10 mM $BaCl_2$; iii) 10 mM BaO_2 NPs. Afterwards, these solutions were moved to quartz capillary columns and measured by a Bruker EMX-8/2.7 spectrometer at room temperature. The above procedures were operated in the dark.

6. Measuring the hydroxyl radical yield using coumarin as fluorescence probe

Coumarin is a highly efficient hydroxyl radical scavenger, which could react with hydroxyl radical and become fluorescent hydroxycoumarin. To confirm the optimal excitation wavelength, 200 μL of deionized water who mixed with 10 μL of coumarin (0.1 M, dissolved

in alcohol) was subjected to UV irradiation for 24h, and the excitation spectrum was measured using a Spectro fluorometer (emission wavelength: 456 nm). To ensure the sustainable fluorescence enhancement of coumarin who suffering with different degrees of oxidation, 5 μL of different concentrations of H_2O_2 (0 mM, 40 mM, 200 mM, 400 mM) were added to the 200 μL of aqueous solution containing 1 μmol coumarin, followed by an extra irradiation of UV light for 3 h. The fluorescence intensities were then examined.

To study the hydroxyl radical yield of BaO_2 NPs after the X-ray radiation, 10 μL of coumarin (0.1 M, dissolved in alcohol) were mixed with 200 μL of the following solutions and subjected to varied X-ray radiation: i) deionized water and 5 Gy of radiation; ii) 50 μg/mL H_2O_2 and 5 Gy of radiation; iii) 50 μg/mL $BaCl_2$ and 5 Gy of radiation; iv) 50 μg/mL BaO_2 NPs; v) 50 μg/mL BaO_2 NPs and 5 Gy of radiation; vi) 100 μg/mL BaO_2 NPs and 5 Gy of radiation; vii) 100 μg/mL BaO_2 NPs and 10 Gy of radiation. Afterwards, the solutions were centrifuged and the supernatants were diluted to 2 mL to proceed with fluorescence measurement (excitation wavelength: 348 nm). The fluorescence intensities at 510 nm were picked out to make the comparing.

Moreover, the radiation-dose-dependent hydroxyl radical yield of BaO_2 NPs were also explored. 50 μg/mL BaO_2 NPs (dispersed in deionized water) and 2 mL of coumarin (10 mM, dissolved in deionized water) were mixed together and then subjected to different X-ray radiation dose (0, 4, 8, 12, 16, 20 Gy). Afterwards, the solutions were centrifuged, and 2 mL of supernatants were pipetted out to proceed with fluorescence measurement (excitation wavelength: 348 nm). The fluorescence intensities at 455 nm were marked as F_i, where i represented the exact radiation dose. The fluorescence changes (Fc, %) were calculated using the following formula: $Fc = (F_i-F_0)/F_0$

7. The study of structural destruction of GLDA by hydroxyl radical

0.2 mmol of GLDA aqueous solution was mixed with 10 mmol H_2O_2 and subjected to UV light irradiation for 4 h, and the solution was then put in an oven (60℃) for another 12 h to remove the extra H_2O_2. After removing the water using a freeze dryer, the residue was dissolved in deuterium oxide and HNMR was detected. The GLDA solution without UV light irradiation was set as control.

To study the complexing ability changes of GLDA with Ba^{2+} before/after the degradation, 10 μmol of GLDA aqueous solution was oxidized in advance by H_2O_2 and UV light. After added with 10 μL of $BaCl_2$ (1 mol/L), the solution was analyzed by a Liquid Chromatograph Mass Spectrometer (LC-MS). Another solution with fresh GLDA and $BaCl_2$ at the same concentration was also analyzed as a contrast.

8. cell cytotoxicity studies of GL-BaO_2 NPs *in vitro*

The cell cytotoxicity was performed through a standard CCK-8 assay. Basically, 4T1 cells with the concentration of 5×10^3 cells per well were seeded on 96-well cell culture plates and cultured at 37℃ until all the cells adhere to the plate wall. Then, the culture medium was emptied and the wells were refilled with 100 μL of fresh RPMI medium containing varied concentrations of BaO_2 or GL-BaO_2 NPs (0, 50, 100, 200, 300, 400, 600, 800 μg/mL). Afterwards, the cells were incubated for another 24 h, followed by discarding the culture supernatant and washing with PBS once. Finally, CCK-8 solutions (100 μL) were added into each well and cultivated for 1 h before measuring its absorbance at 450 nm. The cell viabilities were calculated in relation to that of control groups. The cell viability of BaO_2 NPs with varied modification proportion of GLDA (The ratio between BaO_2 and GLDA were denote as 5:1, 2:1 and 1:2) were also evaluated. Besides, the cell viability of BaO_2 NPs and GL-BaO_2 NPs for human healthy cells (293T) are detected as well through a standard CCK-8 assay.

To evaluate the cell toxicity of GL-BaO_2 NPs under X-ray radiation, cells seeded on 96-well cell culture plates were treated with different concentrations of GL-BaO_2 NPs (0, 100, 200, 300, 400 μg/mL) for 6 h before subjected to 0, 4 or 8 Gy of X-ray radiation. After another 24 h of incubation, the culture medium was emptied and the wells were washed with PBS once. Finally, 100 μL of CCK-8 solutions were added and cultivated for 1 h before the measurement.

9. Intracellular hydroxyl radical generation of GL-BaO_2 NPs *in vitro*

4T1 cells were seeded on a 20 mm cell culture dish with glass bottom (10^5 cells per well) and incubated overnight at 37℃ to let the cells adhere to the cell slide. After removal of the culture medium, cells were incubated with RPMI medium or 180 μg/mL GL-BaO_2 NPs (dispersed in fresh RPMI medium) and cultivated for another 4 h. Then, cells were washed with

PBS twice and immersed in 10 μM of HPF for 30 min in the dark before washing away the extracellular probe. Immediately, cells were subjected to 4 Gy of X-ray radiation, fixed in methanol and observed through CLSM. Two more groups without X-ray radiation were also set as control.

10. Colony forming assay of GL-BaO_2 NPs

4T1 cells were seeded in 60 mm cell culture dishes and divided into 5 groups. After cultivated overnight at 37℃, the culture mediums were replaced to 180 μg/mL GL-BaO_2 NPs (dispersed in fresh RPMI medium) and incubated for another 24 h before subjected to varied dose of X-ray radiation (0, 2, 4, 6, 8 Gy). Then, the cells in each group were digested, resuspended in fresh RPMI medium and counted before seeded on a 6-well cell culture plate with the exact concentrations. Specifically, the seeding concentrations were 100, 100, 500, 8000, 20000 cells per well from group 1 to group 5, respectively. After another 10 days of incubation, the cells in each group were washed, fixed and stained with Giemsa dye. The colony formation rate was obtained by counting the colonies. The assessment of the colony forming ability when treating with/without 180 μg/mL BaO_2 NPs (dispersed in fresh RPMI medium) were also applied as control in accordance with the above procedure.

11. Comet assay of GL-BaO_2 NPs

4T1 cells were seeded in 60 mm cell culture dishes and cultivated overnight at 37℃. Then the culture mediums were replaced to 180 μg/mL GL-BaO_2 NPs (dispersed in fresh RPMI medium) or fresh RPMI medium, and incubated for another 6 h before subjected to 4 Gy of X-ray radiation. Finally, cells were digested and harvested, and the standard single cell gel electrophoresis procedure were employed to observe the DNA damage. Two more groups (fresh RPMI medium, 180 μg/mL GL-BaO_2 NPs) without X-ray radiation were also done as control.

12. Cell apoptosis assessment of GL-BaO_2 NPs

4T1 cells were seeded on 6-well cell culture plates and incubated overnight at 37℃ to let the cells adhere to the wall. Then, the culture mediums were discarded, followed by the addition

of the fresh RPMI medium or 180 μg/mL GL-BaO_2 NPs (dispersed in fresh RPMI medium) and treated for another 6 h before subjected to 4 Gy of X-ray radiation. After a further 2 h of culture, all the cells were digested and harvested, and gently washed twice with PBS. Finally, the cells were dyed with annexin V-FITC (5 μL) and propidium iodide (10 μL) and monitored using a flow cytometer. Two more groups (fresh RPMI medium, 180 μg/mL GL-BaO_2 NPs) without X-ray radiation were also set as control.

13. Cell membrane potential detection using fluorescence probe DiSBAC2(5)

DiSBAC2(5) is a membrane-potential sensitive fluorescence dye, in which the relative fluorescence intensity changes can manifest cell membrane potential shifts. More specifically, an increase in relative fluorescence intensity suggest depolarization, whereas a reduction suggest hyperpolarization. Basically, 4T1 cells were seeded on a 20 mm cell culture dish with glass bottom (10^5 cells per well) and incubated overnight at 37℃ to let the cells adhere to the cell slide. After removal of the culture medium, cells were immersed in DiSBAC2(5) for 20 min in the dark before washing away the extracellular probe. Then, cells were cultivated in a live-cell incubator under CLSM to acquire time-series images (imaged every 15 minutes) before and after the addition of fresh RPMI medium, $BaCl_2$ solutions, BaO_2 NPs or GL-BaO_2 NPs (Ex=640 nm). Finally, the acquired images were measured with fluorescence intensities by an ImageJ software and calculated the relative fluorescence intensity change.

14. Biosafety and blood half-life assessment of GL-BaO_2 NPs *in vivo*

All animal experiment procedures were according to the guidelines of the Institutional Animal Care and Use Committee of East China Normal University. Kunming mice and BALB/c mice were purchased and kept at the Laboratory Animal Center of East China Normal University. 12 Kunming mice (about 10 weeks old) were randomly divided into four groups. In the 30-day experimental period, the mice of group 1, 2, 3 were tail intravenously injected with 100 μL of GL-BaO_2 NPs (45 mg/kg, measured by Ba^{2+} content, dispersed in normal saline) on day 1, day 20 and day 27, respectively. The mice of group 4 were tail intravenously injected with 100 μL of normal saline on day 29 as control (all mice received one injection). Finally,

the blood of each mouse in groups was obtained on the 30th day for blood and biochemical analysis; and all mice were sacrificed, the major organs were dissected for H&E staining and histological analysis.

For blood half-life assessment, 3 Kunming mice were tail intravenously injected with 100 μL of GL-BaO_2 NPs (20 mg/kg). Before the injection and at varied times after the injection, 5 μL of blood were taken out and stored in anticoagulant. Then, 4 mL of aqua regia solution was mixed in for several days until the contents were completely dissolved. The Ba^{2+} concentrations were obtained using an ICP-OES and the blood half-life curve was fitted out according to the first-order kinetic drug metabolism process mechanism.

15. *in vivo* treatment evaluation of GL-BaO_2 NPs

the subcutaneous xenograft tumor models were established by implanting the 4T1 cells (10^6 cells per mouse) into the armpits of the female BALB/c mice (about 8 weeks old). After the tumor volume reached 80-100 mm^3, these mice were randomly divided into four groups, and mice in each group were processed with one of the followings: i) intratumorally injection of 20 μL normal saline as control; ii) intratumorally injection of 20 μL normal saline and subjected to 6 Gy of X-ray radiation 5 h later; iii) intratumorally injected with 20 μL GL-BaO_2 NPs (10 mg/kg, measured by Ba^{2+} content, dispersed in normal saline); iv) intratumorally injected with 20 μL GL-BaO_2 NPs (10 mg/kg) and subjected to 6 Gy of X-ray radiation 5 h later. Then, the tumor size and body weight of mice in each group were recorded and photographed every two days in the following 15 days (all mice received only one injection). The tumor volume was calculated by the following formula: $V=L\times W^2/2$, in which L and W stand for the maximum tumor length and width. The relative tumor volume in each mouse was obtained by dividing by the tumor volume on the first day, and the statistical analysis was performed in every group, in which the error bar denoted to the standard deviation of the relative tumor volume. Besides, 24 h after the injection, one mouse was randomly selected from each group and sacrificed to get the tumor tissues for H&E staining. And on the last day of the experimental period, all mice were sacrificed, and the tumor tissues were separated to make a photoshoot.

Supporting Discussion

1. Effect of precursor selection on the morphology and size of BaO_2 nanoparticles

During the preparation of BaO_2 nanoparticles, the addition of organic ligand can greatly affect the growth rate and confine the growth orientation of nanocrystals. Consequently, the gained products show varied particle size and morphology. Specifically, when using free Ba^{2+} as precursor, we can get submicron sized BaO_2 particles. But if replaced with formate-coordinated Ba^{2+} as precursor, bamboo-structured BaO_2 nanocrystals will be formed.

Introducing carboxylic ligands which have a certain coordination ability with Ba^{2+} in the reaction can effectively limit the growth of crystals, thereby obtaining nanosized BaO_2 particles. During the reaction, a ligand exchange process is needed to form crystal nucleus, and the surface capped carboxylic groups can further act as surfactants to limit grain growth. This growth mechanism of nanoparticles has been clearly elucidated in previous studies, such as gold and silver nanoparticles and so on[1-5].

As shown in *Figure S1,* we also attempt to prepare BaO_2 particles using citric- or EDTA-coordinated Ba^{2+} as precursor. From formate to citric to EDTA, the coordination ability with Ba^{2+} become stronger, the product become smaller, attributing to the increased carboxylic ligands that limit crystal growth. But for EDTA-coordinated Ba^{2+}, the coordination ability become too strong to achieve the ligand exchange process. As a result, BaO_2 crystal nuclei cannot be formed.

2. The stability of GL-BaO_2 NPs within two weeks

The stability of GL-BaO_2 NPs within two weeks have been studied. First, the hydrodynamic diameter of GL-BaO_2 NPs are measured within two weeks to investigate their physical stability. As shown in *Figure S5a and S5b*, the hydrodynamic size distributions are relatively narrow and almost unchanged, and the average diameter changes no more than 15 nm within two weeks, demonstrating their good stability in water. Then, GL-BaO_2 NPs are dispersed in pH buffer to evaluate its chemical stability under physiological conditions. *Figure S5c* shows that there is not more than 20% of free Ba^{2+} release during two weeks, and the same with the release of H_2O_2. Moreover, TEM image also demonstrate that the morphology and size

of NPs are not changed at the end of two weeks (*Figure S5d*). The results further suggest that GL-BaO_2 NPs are stable in the physiological environment.

References:

1. Yamamoto, M., Kashiwagi, Y. & Nakamoto, M. Size-Controlled Synthesis of Monodispersed Silver Nanoparticles Capped by Long-Chain Alkyl Carboxylates from Silver Carboxylate and Tertiary Amine. Langmuir 22, 8581-8586 (2006).
2. Hiramatsu, H. & Osterloh, F.E. A Simple Large-Scale Synthesis of Nearly Monodisperse Gold and Silver Nanoparticles with Adjustable Sizes and with Exchangeable Surfactants. Chemistry of Materials 16, 2509-2511 (2004).
3. Bastús, N.G., Merkoçi, F., Piella, J. & Puntes, V. Synthesis of Highly Monodisperse Citrate-Stabilized Silver Nanoparticles of up to 200 nm: Kinetic Control and Catalytic Properties. Chemistry of Materials 26, 2836-2846 (2014).
4. Cushing, B.L., Kolesnichenko, V.L. & O'Connor, C.J. Recent Advances in the Liquid-Phase Syntheses of Inorganic Nanoparticles. Chemical Reviews 104, 3893-3946 (2004).
5. Kim, Y. et al. Syntheses of monodispersed SnO_2 and CeO_2 nanoparticles through the self-capping role of 2-ethylhexanoate ligands. New Journal of Chemistry 31, 260-264 (2006).

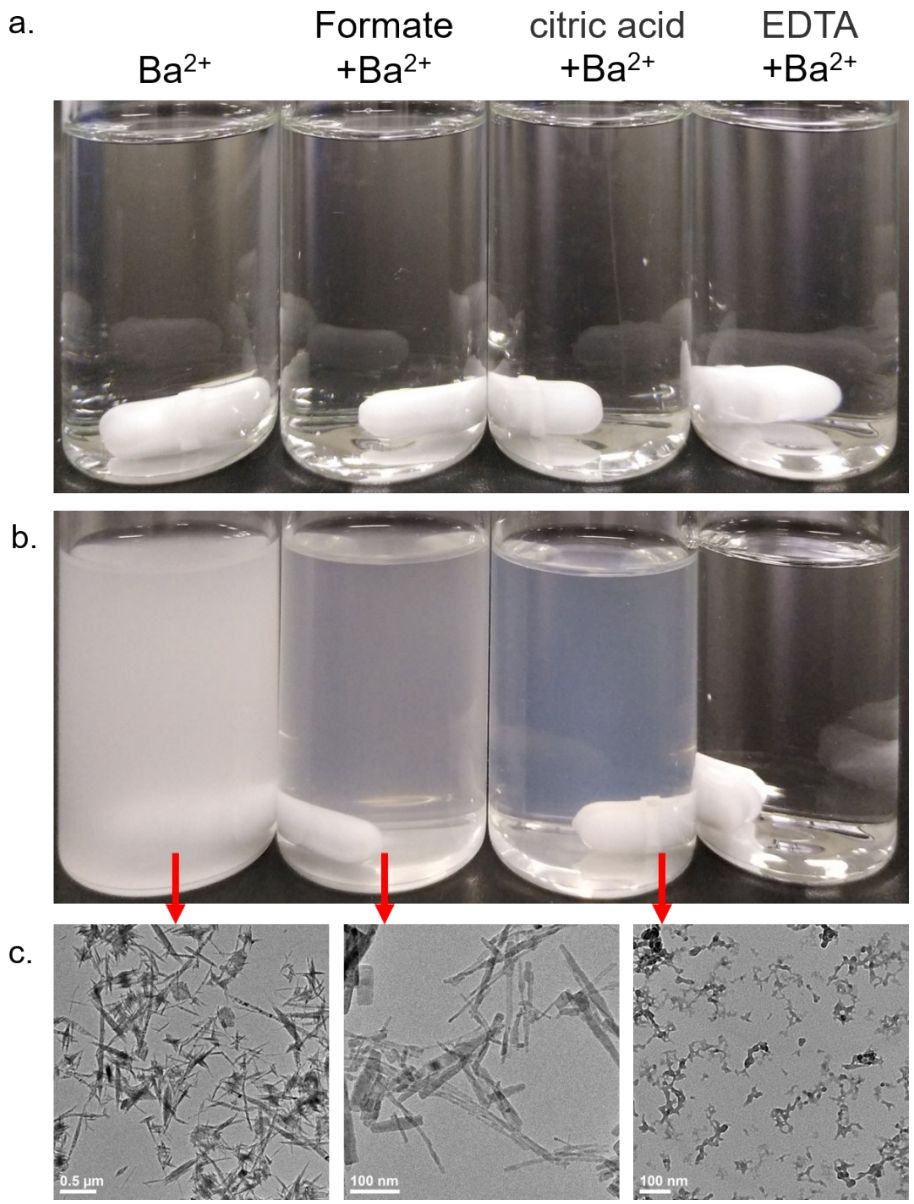

Figure S1: Preparation of BaO_2 particles using different ligand-coordinated Ba^{2+} as precursor. **a,** Before the reaction, all the solutions are clear and transparent. **b,** After the reaction, the turbidity and transparency of the solution become different. **c,** TEM images of the formed BaO_2 particles. When employed with free barium ions as precursor, long rod-shaped BaO_2 particles with submicron size are produced. When employed with formate chelated barium ions as precursor, bamboo-structured BaO_2 nanoparticles are prepared. When employed with EDTA chelated barium ions as precursor, no nanosized product is formed.

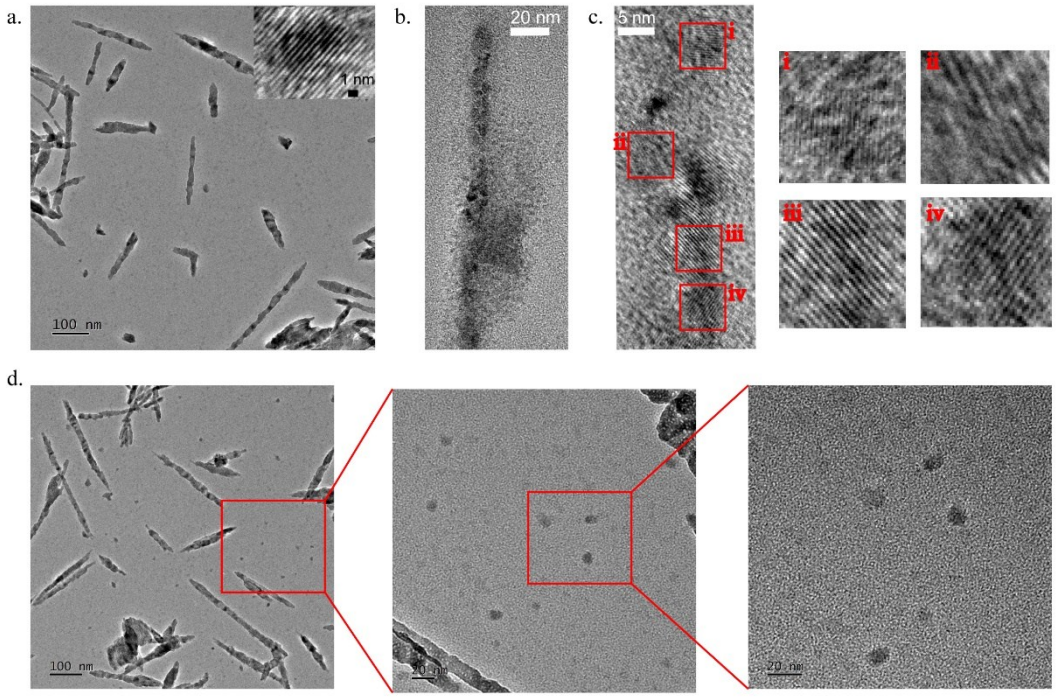

Figure S2: The formation process of BaO_2 crystals observed by TEM. **a,** the full-grown state of bamboo-structured BaO_2 crystals (inserted with high resolution TEM image). **b,** The growing state of BaO_2 crystal with large amounts of nanodots accumulation. **c,** A bamboo-structured BaO_2 crystal with different lattice orientations. **d,** The scattered nanodots beside BaO_2 crystals. The results suggest that the bamboo-structured BaO_2 nanocrystals were formed with nanodots assembling and crystallization.

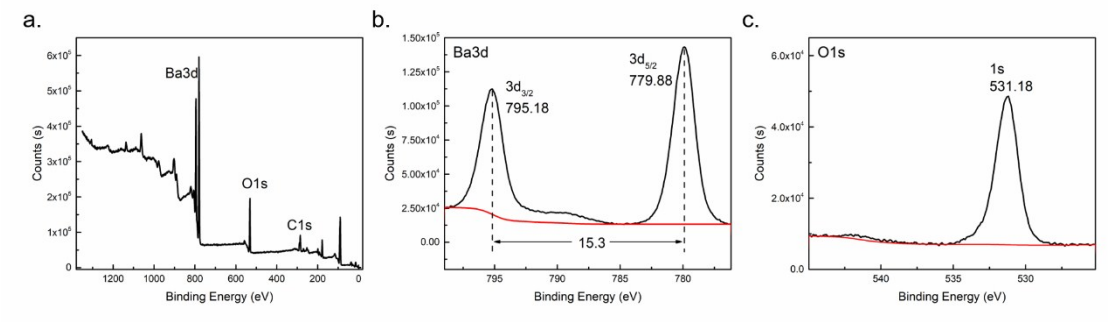

Figure S3: The XPS analysis of BaO_2 NPs. **a,** an overview of XPS spectra of BaO_2 NPs. **b,** XPS spectra of Ba (3d). **c,** XPS spectra of O (1s).

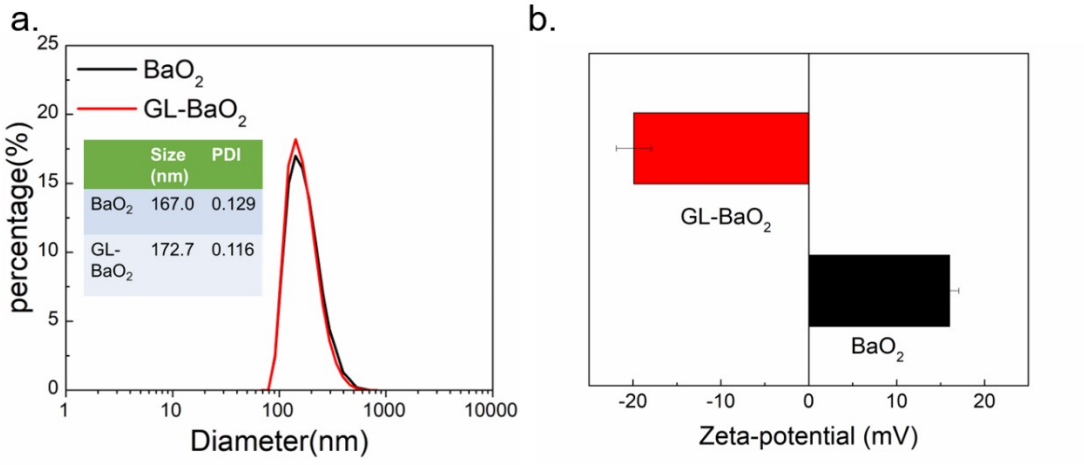

Figure S4: **a,** The hydrodynamic radius of BaO_2 NPs and GL-BaO_2 NPs. **b,** Zeta-potential changes of BaO_2 NPs and GL-BaO_2 NPs.

a.

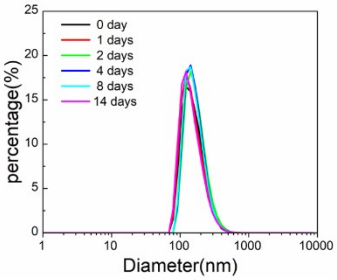

c.

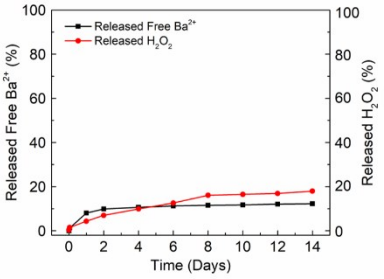

d.

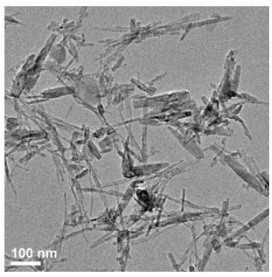

b.

Time (days)	0	1	2	4	8	14
Average Size (nm)	165.5	163.8	157.6	172.7	164.5	151.1
PDI	0.097	0.110	0.145	0.116	0.102	0.127

Figure S5: **a,** size distribution of GL-BaO_2 NPs at different times within two weeks. **b,** average diameters and PDI of GL-BaO_2 NPs at different times within two weeks. **c,** free Ba^{2+} and H_2O_2 release of GL-BaO_2 NPs in pH 7.2 buffer. **d,** TEM image of GL-BaO_2 NPs observed at the end of two weeks.

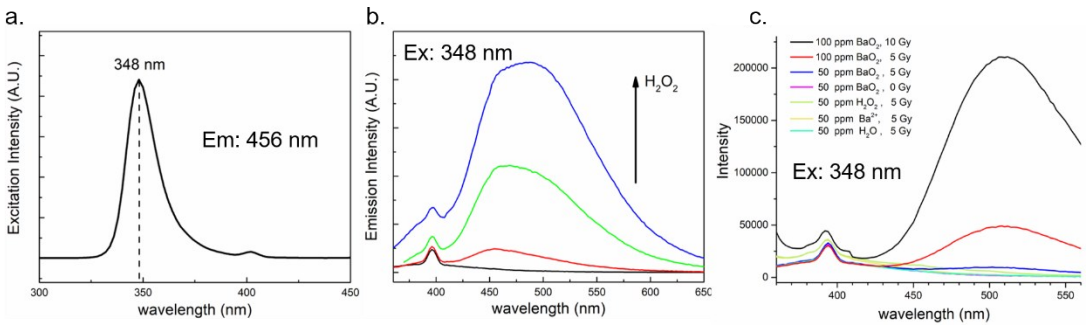

Figure S6: **a,** the excitation spectrum of coumarin after the UV irradiation for 24h. **b,** the emission spectrums of coumarin after suffered with different concentrations of H_2O_2 and UV light irradiation, verifying its sustainable fluorescence enhancement oxidized by hydroxyl radical. **c,** the emission spectrums of coumarin after mixed with H_2O, $BaCl_2$, H_2O_2 or BaO_2 NPs and subject to different radiation dose.

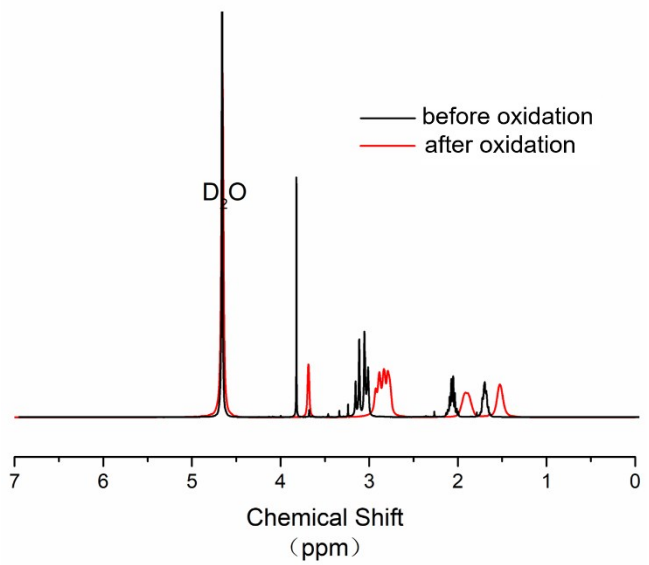

Figure S7: H^1-NMR characteristic spectra of chelator GLDA before and after the oxidation, verifying its structural destruction by hydroxyl radical.

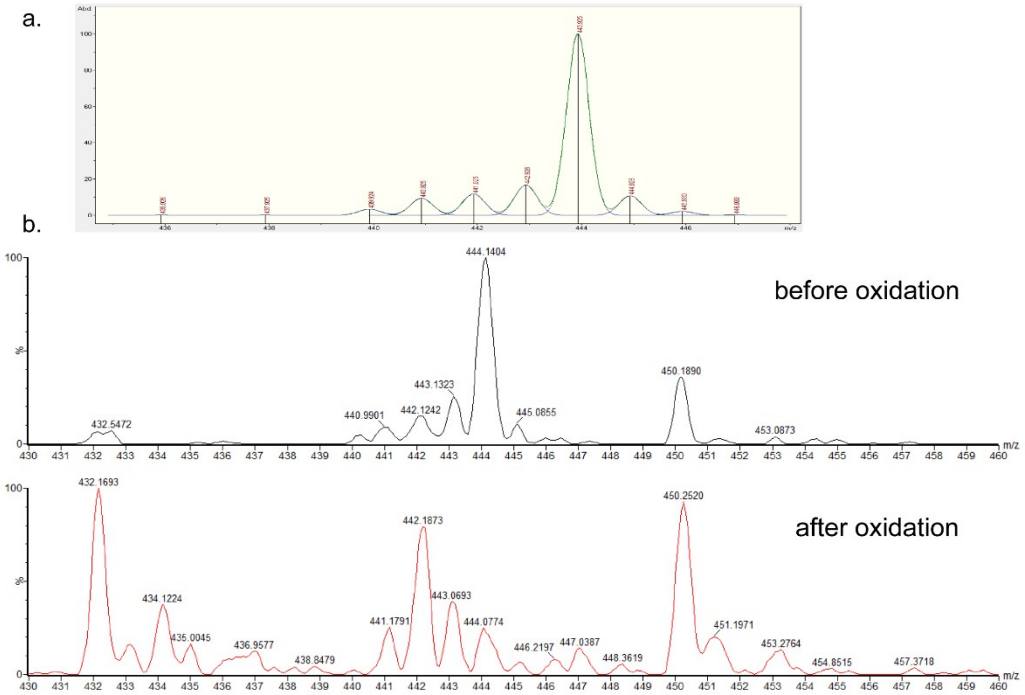

Figure S8: **a,** calculated isotope peaks of Ba-containing molecule in mass spectra. **b,** Mass spectra of GLDA chelated Ba^{2+} solution before and after the oxidation. The peak at m/z=444 before oxidation represents that one GLDA molecule couples one barium ion. The results validate the degradation of GLDA molecules and thus no longer capturing free Ba^{2+}.

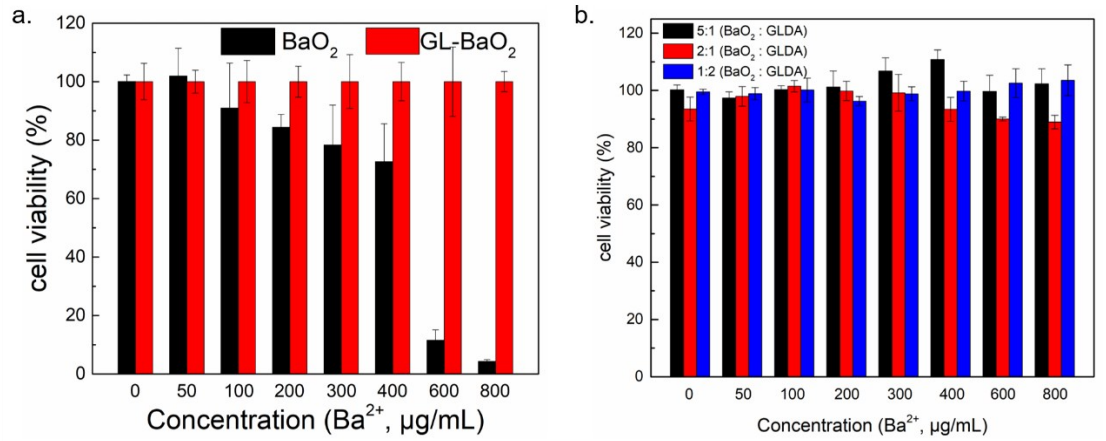

Figure S9: **a,** Cell viability assays when treated 293T cells with different concentrations of BaO_2 or GL-BaO_2 NPs. **b,** 4T1 cell viability assays after the treatment of GL-BaO_2 NPs with varied modification proportion of GLDA. The result suggests that slight GLDA modification can greatly reduce the cytotoxicity of BaO_2 NPs.

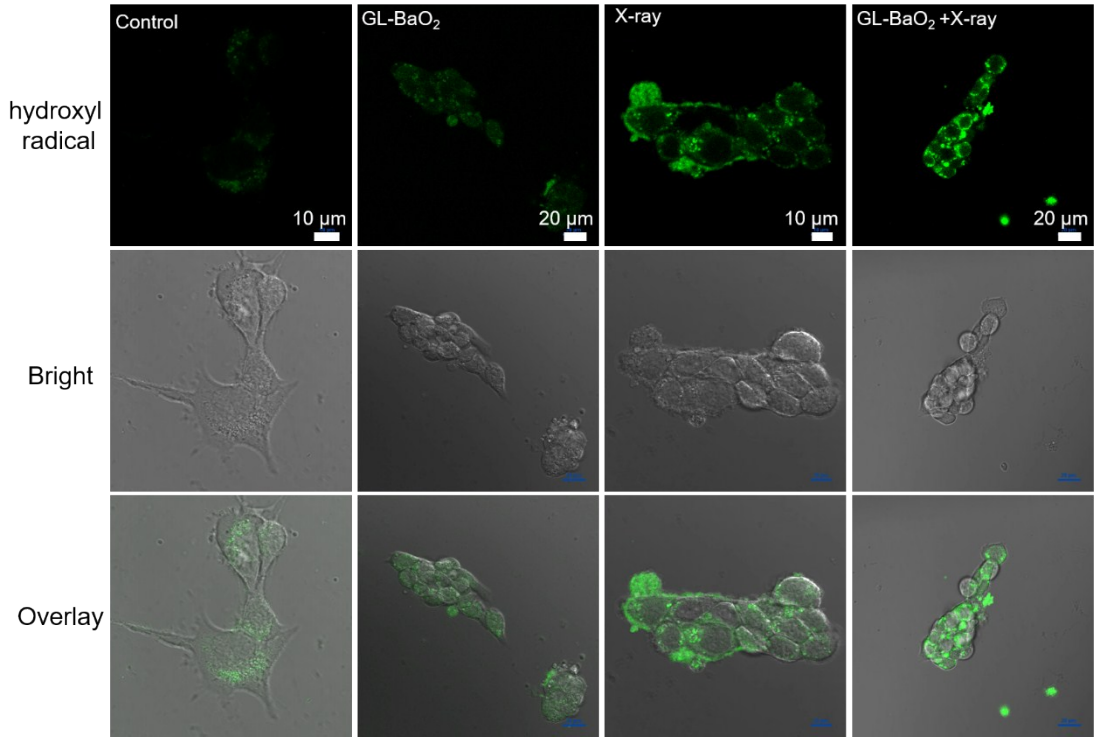

Figure S10: Intracellular hydroxyl radical production after the treatment with/without X-ray radiation.

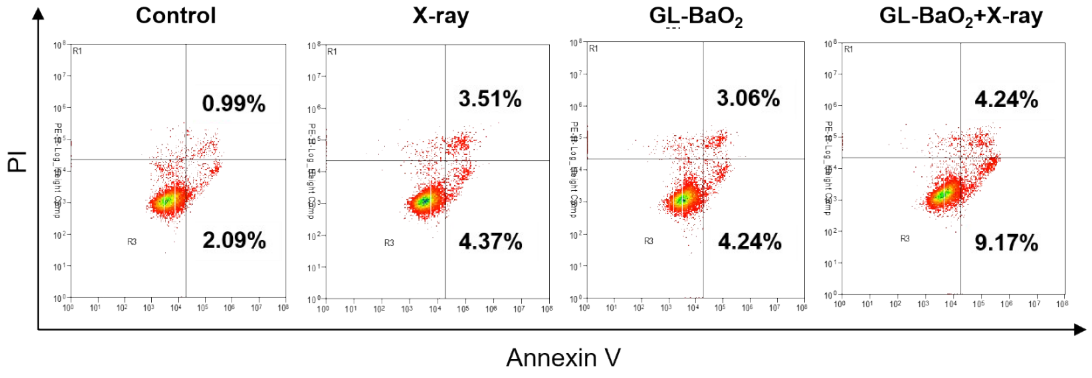

Figure S11: Cell apoptosis assays after incubated with PBS or GL- BaO_2 NPs and then subjected with/without X-ray radiation.

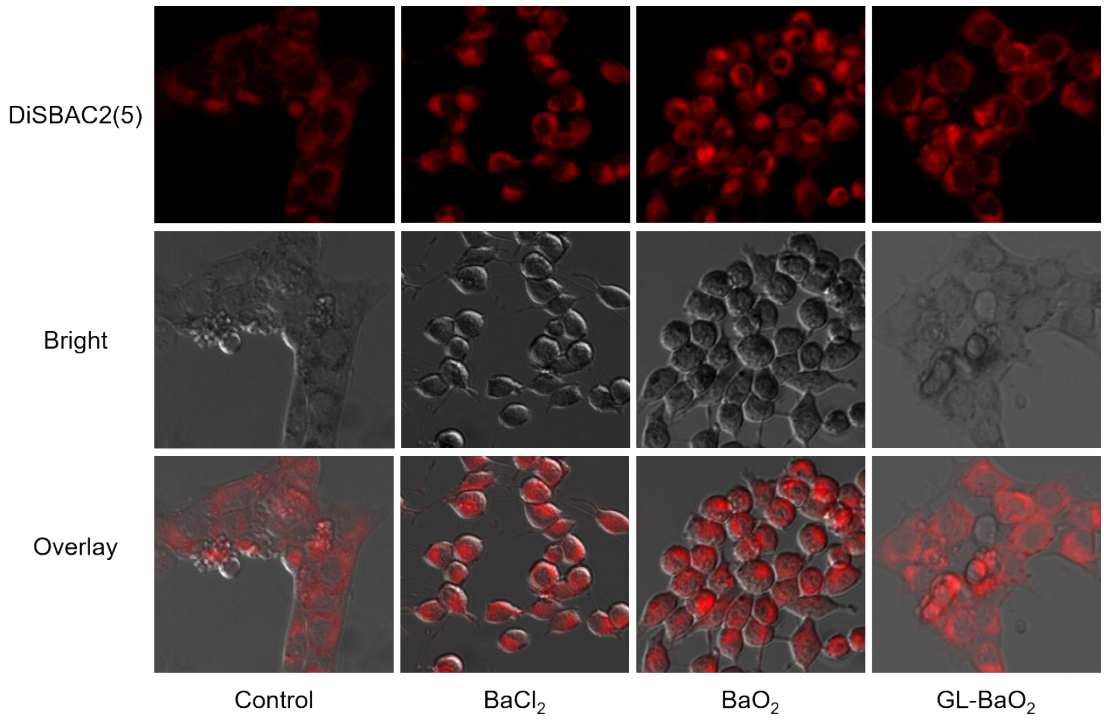

Figure S12: the relative fluorescence intensities after treated cells with fresh RPMI medium, $BaCl_2$ solutions, BaO_2 NPs or GL-BaO_2 NPs. As the relative fluorescence intensity changes can manifest cell membrane potential shifts, the results advise the depolarization of cells after the BaO_2 NPs treatment.

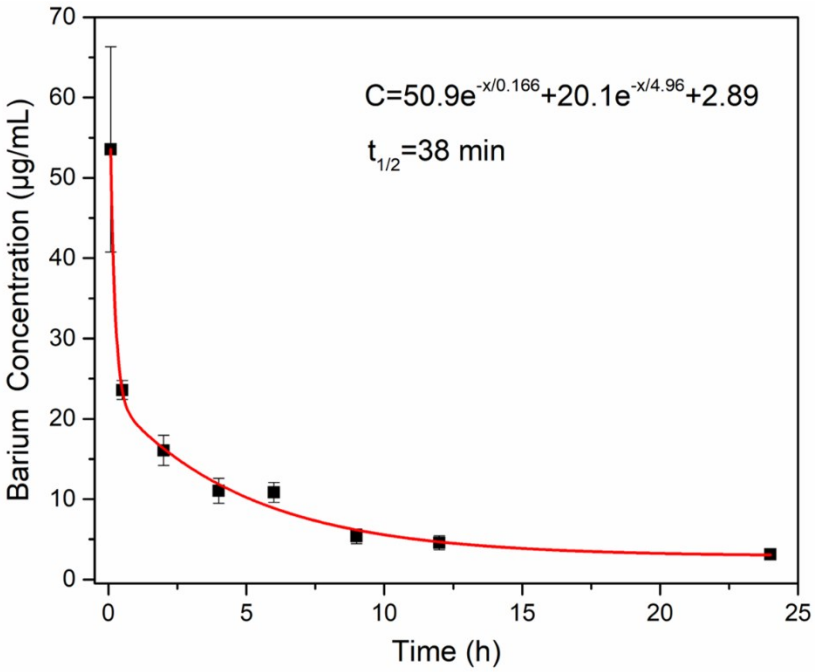

Figure S13: Time-dependent concentrations of Ba in the blood of mice after the intravenous injection of GL-BaO_2 NPs. The blood half-life is calculated as 38 min.

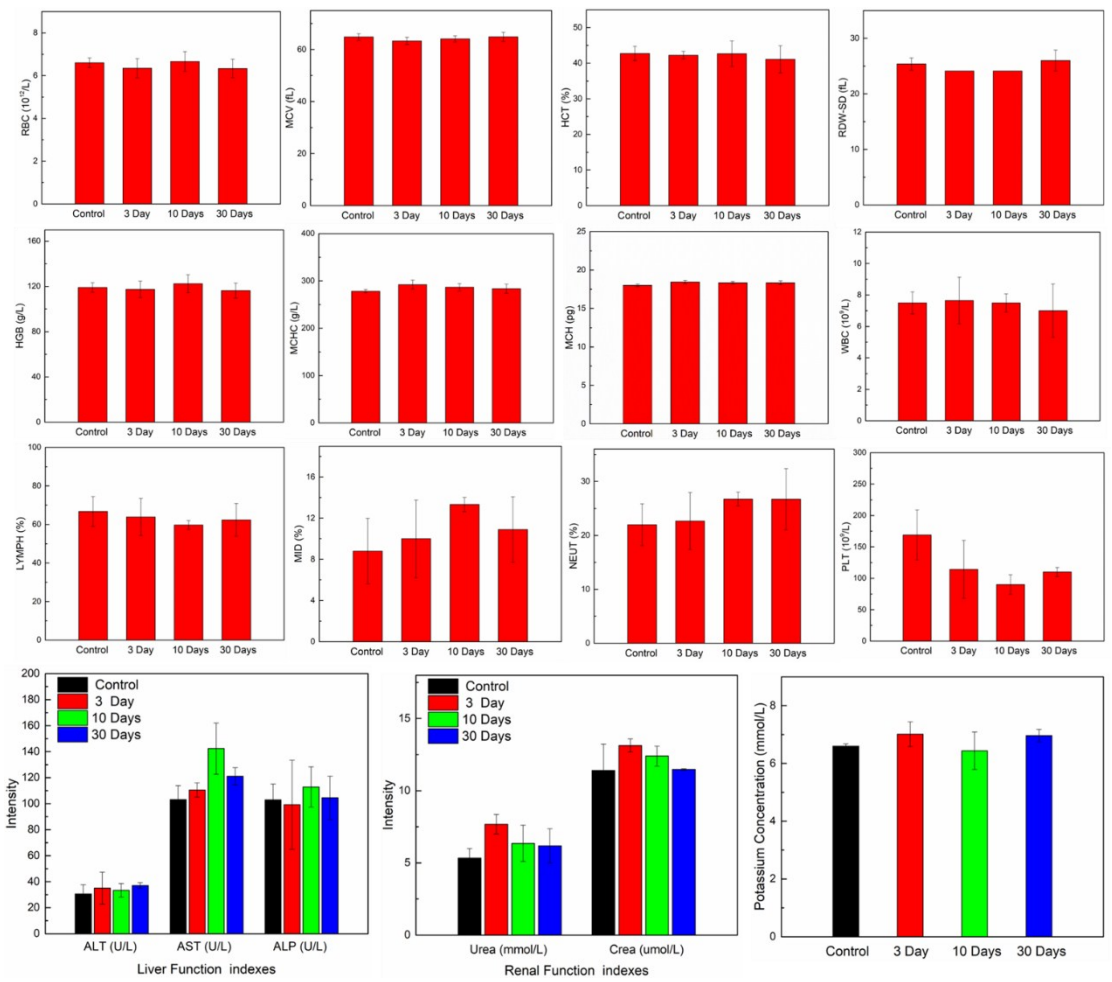

Figure S14: The blood and biochemical analysis of mice. Blood samples are gained on 3th day, 10th day and 30th day after the intravenous injection of GL-BaO_2 NPs, another group of mice are set as control.

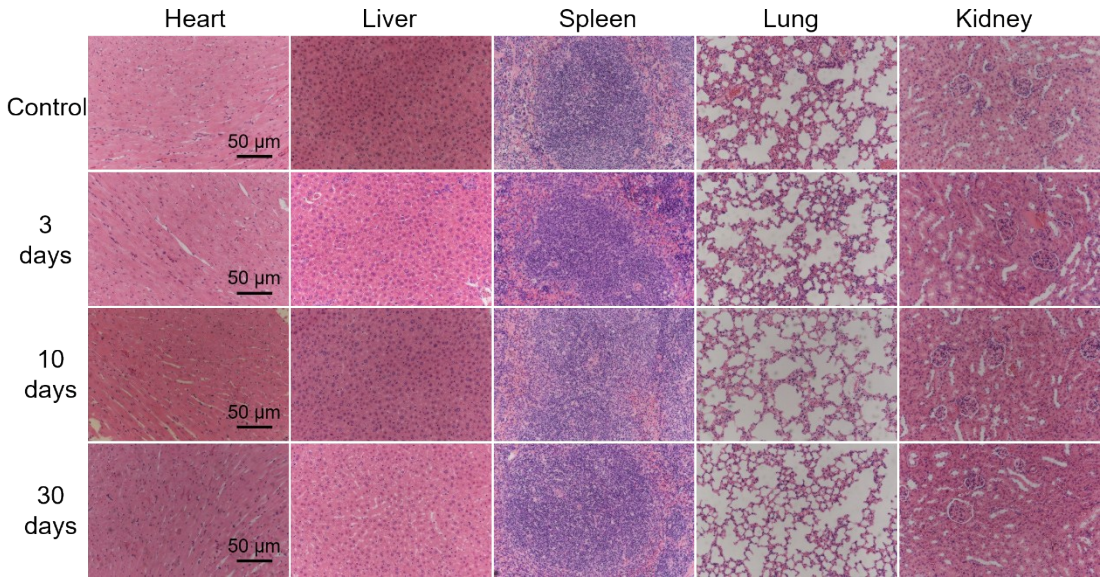

Figure S15: H&E staining of the main organ sections in mice. Mice are dissected on 3th day, 10th day and 30th day after the intravenous injection of GL-BaO_2 NPs, another group of mice are set as control.

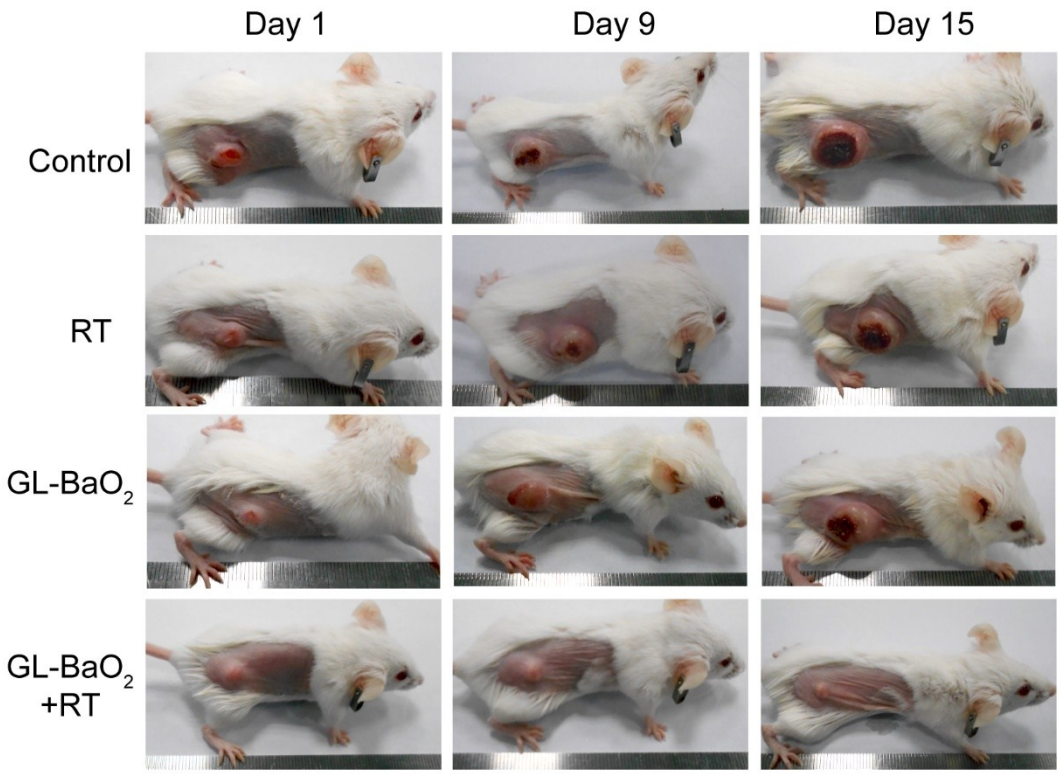

Figure S16: Digital photographs of one mouse in each group on the day 1, day 9 and day 15 after different treatment.